

Fully oxygenated water columns over continental shelves before the Great Oxidation Event

Chadlin M. Ostrander^{1,2*}, Sune G. Nielsen^{1,2,3}, Jeremy D. Owens⁴, Brian Kendall⁵,
Gwyneth W. Gordon¹, Stephen J. Romaniello¹ and Ariel D. Anbar^{1,6}

Late Archaean sedimentary rocks contain compelling geochemical evidence for episodic accumulation of dissolved oxygen in the oceans along continental margins before the Great Oxidation Event. However, the extent of this oxygenation remains poorly constrained. Here we present thallium and molybdenum isotope compositions for anoxic organic-rich shales of the 2.5-billion-year-old Mount McRae Shale from Western Australia, which previously yielded geochemical evidence of a transient oxygenation event. During this event, we observe an anticorrelation between thallium and molybdenum isotope data, including two shifts to higher molybdenum and lower thallium isotope compositions. Our data indicate pronounced burial of manganese oxides in sediments elsewhere in the ocean at these times, which requires that the water columns above portions of the ocean floor were fully oxygenated—all the way from the air–sea interface to well below the sediment–water interface. Well-oxygenated continental shelves were probably the most important sites of manganese oxide burial and mass-balance modelling results suggest that fully oxygenated water columns were at least a regional-scale feature of early Earth’s oceans 2.5 billion years ago.

The extent of dissolved O₂ accumulation in Earth’s oceans before the Great Oxidation Event (GOE, ~2.4 to 2.3 billion years ago (Ga); ref. ¹) remains poorly understood. Multiple lines of geochemical evidence indicate that O₂ was produced by cyanobacteria in the surface ocean well before accumulating in the atmosphere during and after the GOE^{2–8}. Models indicate that cyanobacteria in the surface ocean were capable of promoting mild accumulation of dissolved O₂ (up to 25 μM)⁹ in shallow waters under a predominantly anoxic atmosphere, perhaps extending across large areas of the ocean¹⁰. However, it is difficult to test these models because existing geochemical proxies cannot easily be used to assess the breadth and depth of ocean oxygenation.

A case has been made for widespread oxygenation of shallow waters before the GOE in continental margin environments on the basis of carbon isotopes in bulk rock and kerogen from 2.7 Ga carbonate sedimentary rocks². However, this earlier work could not determine whether O₂ accumulation was restricted to surface waters or extended deeper in the water column, let alone whether oxygenation reached bottom waters and sediments (that is, a fully oxygenated water column).

A fully oxygenated water column at 2.6–2.5 Ga was inferred from black shales (upper Nauga Formation, Ghaap Group, South Africa) enriched in Re but not Mo relative to average crustal abundances³. This geochemical signature occurs when O₂ is present in pore waters at a depth of up to around 1 cm below the sediment–water interface, when Fe(III) becomes the dominant electron acceptor during oxidation of organic matter and sulfide accumulation is low^{11,12} (Fig. 1a). However, this evidence was restricted to a single continental margin (Griqualand West Basin) and could not be extrapolated to the wider oceans.

If fully oxygenated water columns on continental margins were a widespread feature of pre-GOE oceans, then Mn oxide burial

in sediments beneath these settings would also have been widespread. In the modern ocean, O₂ in marine bottom waters and sediments readily oxidizes dissolved Mn(II) and Mn(III) to insoluble Mn(IV)-bearing minerals that precipitate out of solution^{13,14}. In contrast, Mn oxides do not form under anoxic conditions, nor are they buried in anoxic marine sediments. Even if formed under O₂-rich conditions, Mn oxides undergo reductive dissolution shortly after being exposed to anoxic conditions within the water column or sediments^{13–15}. Manganese oxides are highly unstable when O₂ is absent because in such conditions they are an efficient electron acceptor¹⁶. Therefore, appreciable Mn oxide burial today only occurs where water columns are fully oxygenated and O₂ persistently penetrates sediment pore waters¹⁴. In Earth’s past, Mn oxides should have also been buried where O₂ penetrated deeply into marine sediments. This could have occurred under more oxidizing conditions than those identified by Kendall et al.³ in the Nauga Formation shales, where Re abundances are elevated but Mo abundances are negligible. Specifically, Mn oxide burial requires the penetration of O₂ well beyond 1 cm below the sediment–water interface and occurs before Fe(III) becomes the primary electron acceptor during organic carbon oxidation^{14,16} (for example, Fig. 1b).

Here, we pair Tl and Mo isotope data from the late Archaean (~2.5 Ga) black shales of the Mount McRae Shale (Hamersley Basin, Western Australia) to track the extent of marine Mn oxide burial before the GOE. The isotopic cycling of both Tl and Mo in the ocean is directly linked to global Mn oxide burial fluxes^{17,18}. Therefore, their paired application is a powerful way to infer the extent of fully oxygenated water columns at a regional-to-global scale, in contrast to other proxies (such as Re versus Mo enrichments and¹¹ sedimentary Fe speciation¹⁹) that focus only on redox conditions in the local water column.

¹School of Earth and Space Exploration, Arizona State University, Tempe, AZ, USA. ²NIRVANA Laboratories, Woods Hole Oceanographic Institution, Woods Hole, MA, USA. ³Department of Geology and Geophysics, Woods Hole Oceanographic Institution, Woods Hole, MA, USA. ⁴Department of Earth, Ocean, and Atmospheric Science, National High Magnetic Field Laboratory, Florida State University, Tallahassee, FL, USA. ⁵Department of Earth and Environmental Sciences, University of Waterloo, Waterloo, Ontario, Canada. ⁶School of Molecular Sciences, Arizona State University, Tempe, AZ, USA.

*e-mail: cmostran@asu.edu

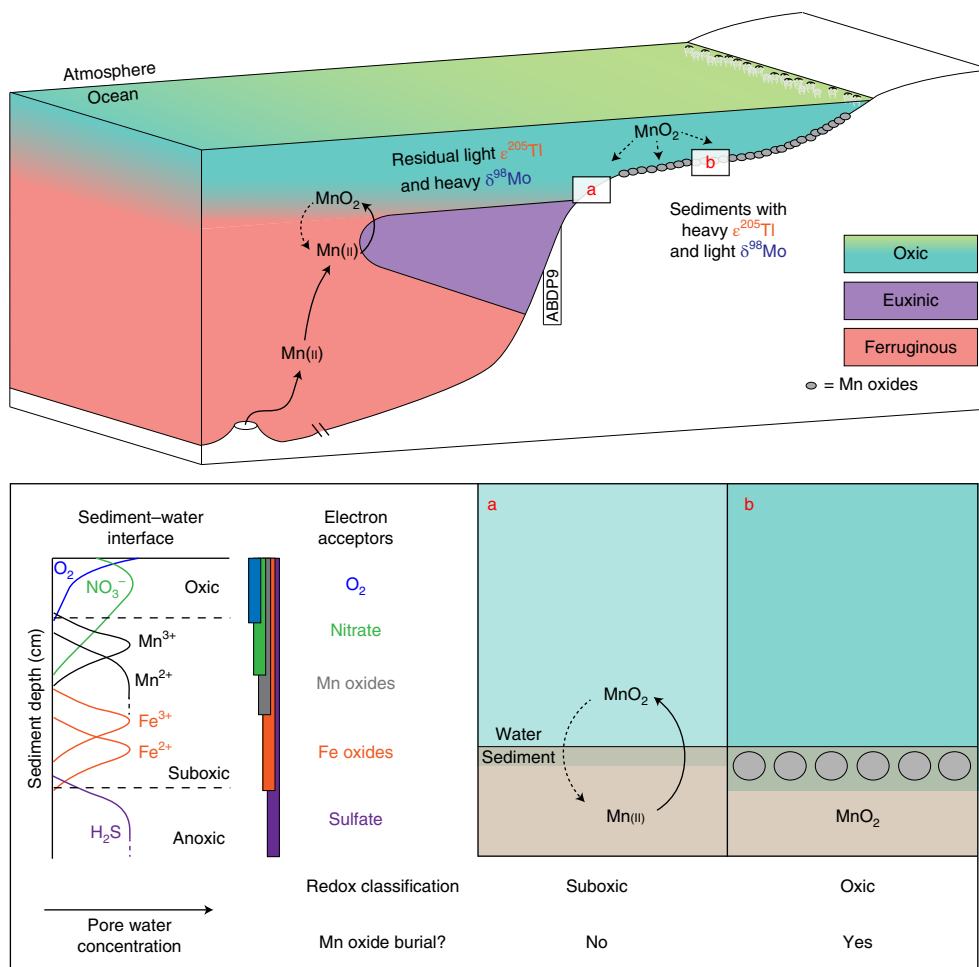


Fig. 1 | Illustration of a possible well-oxygenated marine margin before the GOE. The top diagram depicts a possible marine margin in the Hamersley Basin during deposition of the 2.5 Ga Mount McRae Shale. Evidence exists for sufficient O_2 accumulation in an ancient water column between 2.6 and 2.5 Ga to weakly oxygenate underlying sediments³ (suboxic, depicted in **a**). However, O_2 penetration into these sediments was not sufficient to promote Mn oxide burial^{11,12}. If settings capable of burying Mn oxides were present in ancient oceans over a large seafloor area (oxic, depicted in **b**), then seawater Tl and Mo isotope compositions would have decreased and increased, respectively. The Mount McRae Shale was deposited under locally euxinic conditions³⁷ and should therefore have captured these changes in seawater isotope signatures^{18,28}. Sedimentary redox structure in the lower left-hand corner of the figure summarizes current understanding of the possible electron acceptors present under each redox condition^{16,50}.

Pairing Tl and Mo isotopes to track palaeoredox conditions

The use of Tl isotopes as a palaeoredox proxy is relatively new^{17,20,21}, but builds on extensive earlier study of Tl isotope systematics. The Tl isotope composition of modern seawater (reported in epsilon notation: $\epsilon^{205}\text{Tl}$, where $\epsilon^{205}\text{Tl} = \left(\frac{^{205/203}\text{Tl}_{\text{sample}}}{^{205/203}\text{Tl}_{\text{NIST-997}}} - 1 \right) \times 10^4$) is homogenous and lighter than that of bulk continental crust ($\epsilon^{205}\text{Tl}_{\text{seawater}} = -6.0 \pm 0.3$ (refs. ^{18,22}), compared to $\epsilon^{205}\text{Tl}_{\text{bulk-crust}} = -2.1 \pm 0.3$ (ref. ²³)). The light $\epsilon^{205}\text{Tl}$ in modern seawater is a result of the preferential removal of isotopically heavy Tl from seawater by Mn oxides in well-oxygenated marine sediments²⁴. Importantly, the contemporaneous seawater $\epsilon^{205}\text{Tl}$ signature is captured and preserved in sediments from anoxic and sulfidic (that is, euxinic) basins¹⁸. Tl isotope studies of sedimentary rocks deposited under euxinic conditions therefore provide a means to track ancient seawater $\epsilon^{205}\text{Tl}$ signatures, which should vary in response to changes in Mn oxide burial fluxes. In support of this application, two recent studies used Tl isotope compositions in Mesozoic shales deposited in locally euxinic conditions to track changes in Mn oxide burial fluxes before, during and after oceanic anoxic events, documenting episodes of substantial marine deoxygenation^{20,21}.

Molybdenum isotopes are a more established proxy that has also been shown to be sensitive to marine Mn oxide burial²⁵. The modern

seawater Mo isotope composition (reported in delta notation: $\delta^{98}\text{Mo}$, where $\delta^{98}\text{Mo} = \left(\frac{^{98/95}\text{Mo}_{\text{sample}}}{^{98/95}\text{Mo}_{\text{NIST-SRM-3134}}} - 1 \right) + 0.25\text{‰}$)²⁶ is heavier than that of bulk continental crust ($\delta^{98}\text{Mo}_{\text{seawater}} = 2.34 \pm 0.10\text{‰}$ ²⁶, compared with $\delta^{98}\text{Mo}_{\text{bulk-crust}} = 0.47 \pm 0.12\text{‰}$ (ref. ²⁷)). This heavy seawater $\delta^{98}\text{Mo}$ composition is due largely to the preferential removal of lighter-mass Mo isotopes by adsorption to Mn oxides in well-oxygenated marine sediments²⁵. In a similar way to Tl, this heavy seawater $\delta^{98}\text{Mo}$ value is captured in strongly euxinic settings where Mo removal from bottom waters is quantitative²⁸.

It is useful to measure Tl isotopes in addition to Mo isotopes because Mo isotope interpretation is complicated by alternative fractionation pathways that do not affect Tl isotopes. For example, processes that occur during continental weathering²⁹ and riverine transport³⁰ can remove isotopically light Mo (but see ref. ³¹), yet do not cause measurable Tl isotope fractionation²³. Weakly sulfidic marine sediments also incorporate lighter-mass Mo isotopes²⁸ but impart no known isotopic effect on Tl¹⁸. Iron oxides can remove isotopically light Mo and drive seawater to heavy $\delta^{98}\text{Mo}$ values³², but are unlikely to fractionate Tl isotopes because Fe oxides lack the ability to oxidize Tl(I) to Tl(III), which is what drives isotopic fractionation during sorption to Mn oxides^{24,33}.

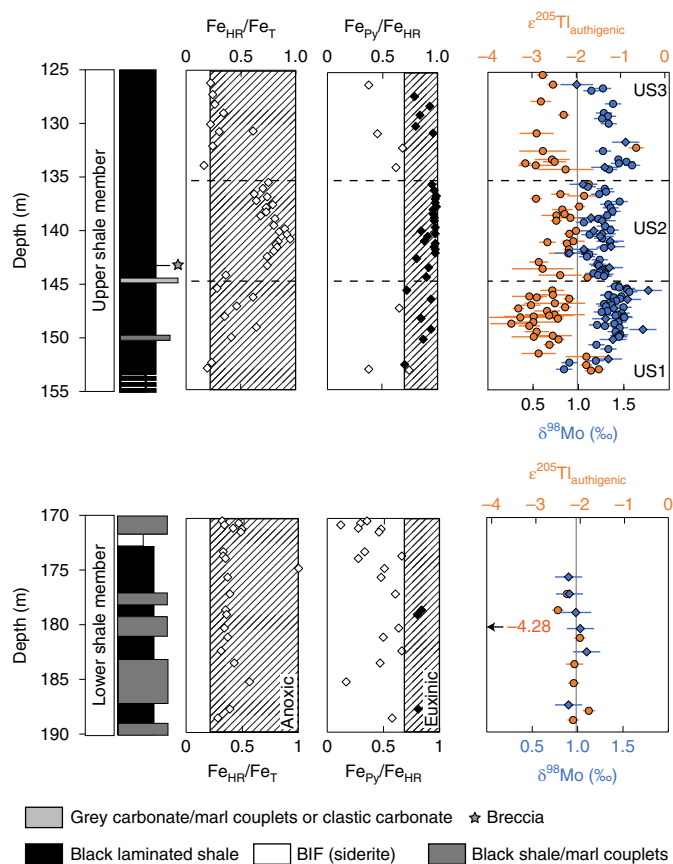


Fig. 2 | Geochemical profiles in organic-rich shales from the Mount McRae Shale. Left: stratigraphic columns for the upper shale member (top) and lower shale member (bottom). Right: geochemical profiles. The hatched boxes represent values indicative of anoxic ($\text{Fe}_{\text{HR}}/\text{Fe}_{\text{T}} > 0.22$, where the HR and T subscripts signify highly reactive and total Fe, respectively) and euxinic ($\text{Fe}_{\text{Py}}/\text{Fe}_{\text{HR}} > 0.7$, where the Py subscript signifies Fe in the form of pyrite) deposition¹⁹. Data that exceed both criteria are in black. Diamonds reflect data from previous work^{37,38} and circles are data from this study. The grey vertical line in the isotope plots represents average isotope compositions from the lower shale member, with the exception of one anomalous Tl isotope value ($\epsilon^{205}\text{Tl} = -4.28 \pm 0.13$ at 180.33 m). All error bars represent the 2 s.d. reproducibility of that sample or the external long-term reproducibility of natural reference materials, whichever is greater.

Anticorrelation of Mo and Tl isotopes in 2.5 Ga shales

We focus on the 2.5 Ga Mount McRae Shale from Western Australia in drill core ABDP9 because black shales from the upper part of this formation host convincing evidence for a widespread oxygenation episode predating the GOE^{5,6,34–40}. These rocks are an ideal archive for tracking fluctuations in seawater Tl and Mo isotope compositions at 2.5 Ga because they were deposited in locally euxinic conditions³⁷ that favour preservation of seawater $\delta^{98}\text{Mo}$ and $\epsilon^{205}\text{Tl}$ values (Fig. 1; see Supplementary Information for more details about the Mount McRae Shale).

Molybdenum isotope signatures much heavier than those of igneous crustal rocks were previously found in the Mount McRae Shale (and in coeval shales from South Africa⁴¹) but could not be definitively ascribed to Mn oxide burial elsewhere in the ocean³⁸. If Mn oxides were being buried at this time, $\epsilon^{205}\text{Tl}$ should also be fractionated relative to bulk continental crust. An anticorrelation between $\epsilon^{205}\text{Tl}$ and $\delta^{98}\text{Mo}$ is expected because fractionation incurred during Mn oxide adsorption occurs in opposing directions for the two isotope systems^{17,18}.

We find that $\epsilon^{205}\text{Tl}$ is systematically lighter during two distinct intervals of the euxinic upper shale (US) member in the Mount McRae Shale: 153.30–144.36 m (US1) and 134.17–126.15 m (US3) (average $\epsilon^{205}\text{Tl} = -2.65$) (Fig. 2 and Fig. 3). $\delta^{98}\text{Mo}$ exhibits heavier values in these same intervals (average $\delta^{98}\text{Mo} = 1.37\text{‰}$), revealing the predicted anti-correlation with $\epsilon^{205}\text{Tl}$. Compared with these intervals, Tl and Mo isotope compositions for 144.26–135.58 m (US2) are heavier (average $\epsilon^{205}\text{Tl} = -2.39$, $P = 0.05$, two-tailed unpaired t -test) and lighter (average $\delta^{98}\text{Mo} = 1.23\text{‰}$, $P \ll 0.05$), respectively. A cross-plot of shale samples with both isotope measurements from the upper shale reveals a statistically significant anti-correlation ($P = 0.01$). In contrast to the euxinic upper shale, isotope compositions are invariant in the non-euxinic lower shale member (170–190 m core depth, see the Supplementary Information for discussion of this interval, and interpretation of concentration data).

Fully oxygenated water columns on continental shelves

Light $\epsilon^{205}\text{Tl}$ and heavy $\delta^{98}\text{Mo}$ in US1 and US3 provide strong evidence for the formation and subsequent burial of Mn oxides elsewhere in the ocean at these times. To drive the observed isotopic trends, water columns must have been fully oxygenated over portions of the ocean floor. It is most likely that Mn oxide burial at 2.5 Ga occurred in shallow oxygenated shelf environments where O_2 produced within the surface ocean by cyanobacteria was capable of being continuously transferred to underlying waters and marine sediments (for example, the environment illustrated in Fig. 1b).

Alternative local basin controls or processes in the sedimentary environment where the Mount McRae Shale was deposited cannot explain the observed isotope trends in the upper shale member. In a modern euxinic basin that is not well connected to the open ocean (that is, the Black Sea), Tl isotopes in the local water column and underlying sediments are heavier than the open-ocean signature¹⁸. If the Hamersley Basin was also not well connected to the open ocean, then the $\epsilon^{205}\text{Tl}$ value of the Mount McRae Shale may have been higher than the open-ocean signature. This would require even lighter seawater $\epsilon^{205}\text{Tl}$ compositions during deposition of US1 and US3, which would then imply an even greater extent of sediment Mn oxide burial elsewhere in the oceans. Furthermore, in modern euxinic settings where Mo is not quantitatively transferred from seawater to sediments, sedimentary $\delta^{98}\text{Mo}$ compositions are always lighter than the coeval seawater signature²⁸. Hence, if Mo removal from euxinic bottom waters in the Hamersley Basin was not quantitative, then seawater $\delta^{98}\text{Mo}$ would be even heavier than observed in the Mount McRae Shale, again implying even more significant sediment Mn oxide burial elsewhere in the ocean.

In theory, the observed Tl and Mo isotope shifts might be alternatively explained by ‘shuttling’ of Tl and Mo bound to oxide minerals formed in oxic surface waters to underlying anoxic waters and/or sediments on Late Archaean continental margins, where these elements could then be captured in euxinic sediments. If so, fully oxygenated water columns would not be required to explain the antithetic shifts in Tl and Mo isotopes recorded in the Mount McRae Shale. However, this notion is not supported by observations in the modern Cariaco Basin, a modern analogue environment where Mn oxides are formed in oxygenated surface waters and subsequently transported to euxinic bottom waters and sediments deeper in the basin⁴². An oxide shuttle should cause $\epsilon^{205}\text{Tl}$ in euxinic sediments to be heavier than in surface oxic seawater²⁴. This is not observed, however. Euxinic sediment $\epsilon^{205}\text{Tl}$ in the Cariaco Basin is instead indistinguishable from overlying seawater (average $\epsilon^{205}\text{Tl}_{\text{euxinic}} = -5.1 \pm 1.3$ (2 s.d.) versus $\epsilon^{205}\text{Tl}_{\text{seawater}} = -5.5 \pm 0.7$ (2 s.d.))¹⁸. One possible explanation for this lack of Tl isotope fractionation is that Tl released by Mn oxide dissolution in sulfidic deep waters is first remixed and rehomogenized with the dissolved Tl pool before Tl capture in pyrite. Regardless, as anoxic sediments in

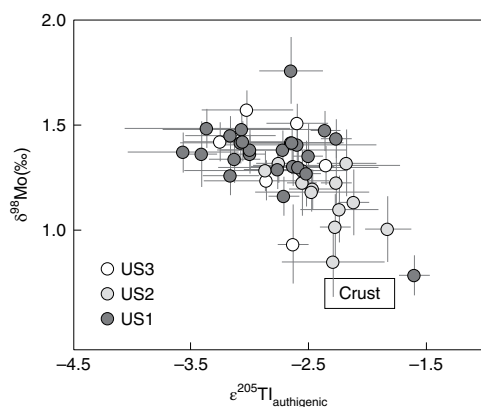


Fig. 3 | Mo and Tl isotope cross-plot from the upper shale member.

The anticorrelation trend in this plot, which is also apparent in Fig. 1, is statistically significant ($P=0.01$). The box indicates current estimates for the isotope compositions of bulk continental crust^{23,27}. All error bars represent the 2 s.d. reproducibility of that sample or the external long-term reproducibility of natural reference materials, whichever is greater.

the modern Cariaco Basin do not preserve the Tl isotope effects of oxide adsorption¹⁸ despite evidence that oxide minerals are delivered at least transiently to these sediments⁴², a Mn oxide shuttle in redox-stratified marine basins probably had a minimal impact on the Late Archaean seawater Tl isotope mass-balance.

Although there are proposed pathways of Mn oxide formation that do not require O_2 , they would not be likely to cause the observed isotopic effects in the upper shale member. Oxidation of reduced Mn in the upper water column by hypothesized Mn-oxidizing phototrophs⁴³ or by ultraviolet light⁴⁴ cannot account for burial at the seafloor because underlying anoxic waters and sediments would recycle Mn back into solution (as Mn(II))^{13,14}. The high abundance of Fe(II) in deep ferruginous waters of the Archaean oceans¹, for example, would readily promote reduction of Mn oxides in anoxic waters. If the water column or sediment pore waters were anoxic, even seasonally¹⁵, reductive dissolution of Mn oxides would release sorbed Tl and Mo. Invoking an O_2 -free explanation for the observed isotopic trends also requires neglecting the many independent lines of evidence for a ‘whiff’ of O_2 at 2.5 Ga^{5,6,34–40}.

Palaeoseawater $\epsilon^{205}\text{Tl}$ and $\delta^{98}\text{Mo}$ values can be estimated directly from the Mount McRae Shale data and used to reconstruct ocean redox conditions. Measured $\epsilon^{205}\text{Tl}$ values serve as a direct estimate for the coeval seawater signature (as low as -3.57 ± 0.48) because euxinic sediments capture the overlying seawater Tl isotope value¹⁸. The $\delta^{98}\text{Mo}$ value recorded in euxinic marine sediments is always equal to or lighter than seawater²⁸, and thus represents a lower limit for the coeval seawater signature (as heavy as $1.56 \pm 0.10\text{‰}$). It is possible, or even likely, that the Tl and Mo isotope compositions of seawater fluctuated during deposition of the upper shale member of the Mount McRae Shale. Deposition of this interval is estimated³⁴ to have occurred over ~ 11 Myr and the whiff of O_2 was probably a transient episode of even shorter duration³⁹. To estimate ocean redox conditions during peak Mn oxide burial, we use the lightest $\epsilon^{205}\text{Tl}$ and heaviest $\delta^{98}\text{Mo}$ values from the upper shale member. During peak Mn oxide burial, the retention of heavier-mass Tl and lighter-mass Mo isotopes would have been maximized, resulting in the lightest $\epsilon^{205}\text{Tl}$ and heaviest $\delta^{98}\text{Mo}$ seawater signatures. Unsurprisingly, the lightest $\epsilon^{205}\text{Tl}$ (-3.57 ± 0.48 at 148.75 m) and heaviest $\delta^{98}\text{Mo}$ ($1.56 \pm 0.10\text{‰}$ at 145.74 m) occur during US1, an interval that hosts multiple lines of geochemical evidence for an oxygenation episode^{5,6,34,37–39}.

Using the estimated seawater $\epsilon^{205}\text{Tl}$ and $\delta^{98}\text{Mo}$ values, ocean redox conditions can be inferred using isotope mass-balance equations as follows:

$$\epsilon^{205}\text{Tl}_{\text{inputs}} = \epsilon^{205}\text{Tl}_{\text{AOC}}(f_{\text{AOC}}) + \epsilon^{205}\text{Tl}_{\text{oxic}}(f_{\text{Tl-oxic}}) + \epsilon^{205}\text{Tl}_{\text{other}}(f_{\text{other}})$$

and

$$\delta^{98}\text{Mo}_{\text{inputs}} = \delta^{98}\text{Mo}_{\text{euxinic}}(f_{\text{euxinic}}) + \delta^{98}\text{Mo}_{\text{SAD}}(f_{\text{SAD}}) + \text{Mo}_{\text{oxic}}(f_{\text{Mo-oxic}})$$

where $\epsilon^{205}\text{Tl}_x$ and $\delta^{98}\text{Mo}_x$ represent the isotopic composition of average oceanic inputs and outputs, and f_x denotes the relative removal flux for each output. For Tl, we designate low-T alteration of oceanic crust (f_{AOC}), well-oxygenated Mn oxide-rich sediments ($f_{\text{Tl-oxic}}$), and other (f_{other}) as the three dominant marine outputs. The other output signifies Tl removal with no associated isotopic fractionation (for example, euxinic basins¹⁸). For Mo, similar to recent work, we use euxinic sediments (f_{euxinic}), sediments that are sulfidic at depth (f_{SAD} ; where sulfide is limited to sediment pore waters), and well-oxygenated Mn oxide-rich sediments ($f_{\text{Mo-oxic}}$) as the three outputs⁴⁵ (see the Supplementary Information for more detailed information about modelling, including key assumptions).

The mass-balance model results indicate that well-oxygenated Mn oxide-rich sediments were an important sink for both Tl ($f_{\text{Tl-oxic}} = 6\text{--}21\%$) and Mo ($f_{\text{Mo-oxic}} = 20\text{--}34\%$) at 2.5 Ga. Together, these results suggest that fully oxygenated shelf environments were a common feature on continental margins, at least regionally, at 2.5 Ga.

We make no attempt here to convert these fluxes into the areal extent of seafloor because the flux per areal unit into these marine outputs was probably much different in the Archaean compared with today. Burial rates of Tl and Mo in modern oxic marine environments that bury Mn oxides are very low, much lower than their burial rates in other modern marine outputs (for example, the burial of Tl during low-T alteration of oceanic crust⁴⁶ and burial of Mo under strong euxinic conditions⁴⁵). For this reason, seafloor area calculations using modern Tl and Mo burial rates and our ancient seawater isotope signature estimates would require the majority of the seafloor at 2.5 Ga to have been oxic. Expansive oxic conditions before the GOE are unlikely because many independent lines of evidence support a predominately anoxic global ocean at this time¹. It is most likely that burial rates of Tl and Mo in 2.5 Ga oxic environments were much higher than today. For example, dissolved Mn concentrations in Archaean seawater may have been four orders of magnitude higher than today⁴⁷, providing a strong potential for high Mn oxide burial rates in oxic environments, and therefore a stronger potential for Tl and Mo adsorption. Furthermore, the burial rate of Mo (and potentially also of Tl) into euxinic environments could have been much lower than today because sulfate concentrations in Archaean oceans were very low⁴⁸. Euxinic conditions in a low-sulfate ocean could have been much weaker than today, lowering the potential for sedimentary retention of Mo. In summary, a smaller area of 2.5 Ga seafloor burying Mn oxides could conceivably drive a more pronounced seawater Tl and Mo isotope signature effect than today, but is difficult to estimate precisely.

Our findings provide a new perspective on marine oxygenation at 2.5 Ga, on the cusp of the GOE. Multiple lines of geochemical evidence provide strong support for O_2 in shallow waters of the Hamersley Basin at 2.5 Ga (refs. 5,6,34) and the adjoining Griqualand West Basin^{4,41} (which may have bordered the same ocean basin⁴⁹). However, because Mn oxide burial requires fully oxygenated water columns at 2.5 Ga, our multi-isotope data supports more oxygenated continental shelves over a greater area than previously

recognized using other geochemical datasets. Specifically, the inferred seawater $\epsilon^{205}\text{Tl}$ and $\delta^{98}\text{Mo}$ composition requires fully oxygenated water columns in shelf environments within the Hamersley Basin and adjoining basin(s), and potentially even large portions of the continental margins worldwide. Our results highlight the important and expanding role of cyanobacteria as engineers of the Archean biosphere, particularly in the run-up to the GOE.

Online content

Any methods, additional references, Nature Research reporting summaries, source data, statements of data availability and associated accession codes are available at <https://doi.org/10.1038/s41561-019-0309-7>.

Received: 20 April 2018; Accepted: 15 January 2019;

Published online: 25 February 2019

References

- Lyons, T. W., Reinhard, C. T. & Planavsky, N. J. The rise of oxygen in Earth's early ocean and atmosphere. *Nature* **506**, 307–315 (2014).
- Eigenbrode, J. L. & Freeman, K. H. Late Archean rise of aerobic microbial ecosystems. *Proc. Natl Acad. Sci. USA* **103**, 15759–15764 (2006).
- Kendall, B. et al. Pervasive oxygenation along late Archean ocean margins. *Nat. Geosci.* **3**, 647–652 (2010).
- Czaja, A. D. et al. Evidence for free oxygen in the Neoproterozoic ocean based on coupled iron-molybdenum isotope fractionation. *Geochim. Cosmochim. Acta* **86**, 118–137 (2012).
- Kendall, B., Brennecka, G. A., Weyer, S. & Anbar, A. D. Uranium isotope fractionation suggests oxidative uranium mobilization at 2.50 Ga. *Chem. Geol.* **362**, 105–114 (2013).
- Stüeken, E. E., Buick, R. & Anbar, A. D. Selenium isotopes support free O_2 in the latest Archean. *Geology* **43**, 259–262 (2015).
- Eickmann, B. et al. Isotopic evidence for oxygenated Mesoproterozoic shallow oceans. *Nat. Geosci.* **11**, 133–138 (2018).
- Koehler, M. C., Buick, R., Kipp, M. A., Stüeken, E. E. & Zaloumis, J. Transient surface ocean oxygenation recorded in the ~2.66-Ga Jeerinah Formation, Australia. *Proc. Natl Acad. Sci. USA* **115**, 7711–7716 (2006).
- Kasting, J. F. In *The Proterozoic Biosphere: A Multidisciplinary Study* (eds Schopf, J. & Klein, C.) 1185–1187 (Cambridge Univ. Press, Cambridge, 1992).
- Olson, S. L., Kump, L. R. & Kasting, J. F. Quantifying the areal extent and dissolved oxygen concentrations of Archean oxygen oases. *Chem. Geol.* **362**, 35–43 (2013).
- Morford, J. L., Emerson, S. R., Breckel, E. J. & Kim, S. H. Diagenesis of oxyanions (V, U, Re, and Mo) in pore waters and sediments from a continental margin. *Geochim. Cosmochim. Acta* **69**, 5021–5032 (2005).
- Morford, J. L., Martin, W. R. & Carney, C. M. Rhenium geochemical cycling: insights from continental margins. *Chem. Geol.* **324–325**, 73–86 (2012).
- Burdige, D. J. The biogeochemistry of manganese and iron reduction in marine sediments. *Earth Sci. Rev.* **35**, 249–284 (1993).
- Calvert, S. E. & Pedersen, T. F. Sedimentary geochemistry of manganese: implications for the environment of formation of manganiferous black shales. *Econ. Geol.* **91**, 36–47 (1996).
- Kristensen, E., Kristiansen, K. D. & Jensen, M. H. Temporal behavior of manganese and iron in a sandy coastal sediment exposed to water column anoxia. *Estuaries* **26**, 690–699 (2003).
- Froelich, P. N. et al. Early oxidation of organic matter in pelagic sediments of the eastern equatorial Atlantic: suboxic diagenesis. *Geochim. Cosmochim. Acta* **43**, 1075–1090 (1979).
- Nielsen, S. G. et al. Thallium isotopes in early diagenetic pyrite—a paleoredox proxy? *Geochim. Cosmochim. Acta* **75**, 6690–6704 (2011).
- Owens, J. D., Nielsen, S. G., Horner, T. J., Ostrander, C. M. & Peterson, L. C. Thallium-isotopic compositions of euxinic sediments as a proxy for global manganese-oxide burial. *Geochim. Cosmochim. Acta* **213**, 291–307 (2017).
- Raiswell, R. et al. The iron paleoredox proxies: a guide to pitfalls, problems and proper practice. *Am. J. Sci.* **318**, 491–526 (2018).
- Ostrander, C. M., Owens, J. D. & Nielsen, S. G. Constraining the rate of oceanic deoxygenation leading up to a Cretaceous oceanic anoxic event (OAE-2: ~94 Ma). *Sci. Adv.* **3**, e1701020 (2017).
- Them, T. R. et al. Thallium isotopes reveal protracted anoxia during the Toarcian (Early Jurassic) associated with volcanism, carbon burial, and mass extinction. *Proc. Natl Acad. Sci. USA* **115**, 6596–6601 (2018).
- Nielsen, S. G. et al. Hydrothermal fluid fluxes calculated from the isotopic mass balance of thallium in the ocean crust. *Earth Planet. Sci. Lett.* **251**, 120–133 (2006).
- Nielsen, S. G. et al. Thallium isotopic composition of the upper continental crust and rivers—an investigation of the continental sources of dissolved marine thallium. *Geochim. Cosmochim. Acta* **19**, 2007–2019 (2005).
- Nielsen, S. G. et al. Towards an understanding of thallium isotope fractionation during adsorption to manganese oxides. *Geochim. Cosmochim. Acta* **117**, 252–265 (2013).
- Wasylenki, L. E. et al. The molecular mechanism of Mo isotope fractionation during adsorption to birnessite. *Geochim. Cosmochim. Acta* **75**, 5019–5031 (2011).
- Nägler, T. F. et al. Proposal for an international molybdenum isotope measurement standard and data representation. *Geostand. Geoanal. Res.* **39**, 149–151 (2014).
- Willbold, M. & Elliot, T. Molybdenum isotope variations in magmatic rocks. *Chem. Geol.* **449**, 253–268 (2017).
- Neubert, N., Nægler, T. F. & Böttcher, M. E. Sulfidity controls molybdenum isotope fractionation into euxinic sediments: evidence from the modern Black Sea. *Geology* **36**, 775–778 (2008).
- Siebert, C. et al. Molybdenum isotope fractionation in soils: influence of redox conditions, organic matter, and atmospheric inputs. *Geochim. Cosmochim. Acta* **162**, 1–24 (2015).
- Archer, C. & Vance, D. The isotopic signature of the global riverine molybdenum flux and anoxia in the ancient oceans. *Nat. Geosci.* **1**, 597–600 (2008).
- King, E. K. & Pett-Ridge, J. C. Reassessing the dissolved molybdenum isotopic composition of ocean inputs: the effect of chemical weathering and groundwater. *Geology* **46**, 955–958 (2018).
- Goldberg, T., Archer, C., Vance, D. & Poulton, S. W. Mo isotope fractionation during adsorption to Fe (oxyhydr)oxides. *Geochim. Cosmochim. Acta* **73**, 6502–6516 (2009).
- Peacock, C. L. & Moon, E. M. Oxidative scavenging of thallium by birnessite: explanation for thallium enrichment and stable isotope fractionation in marine ferromanganese precipitates. *Geochim. Cosmochim. Acta* **84**, 297–313 (2012).
- Anbar, A. D. et al. A whiff of oxygen before the Great Oxidation Event? *Science* **317**, 1903–1906 (2007).
- Kaufman, A. J. et al. Late Archean biospheric oxygenation and atmospheric evolution. *Science* **317**, 1900–1903 (2007).
- Garvin, J., Buick, R., Anbar, A. D., Arnold, G. L. & Kaufman, A. J. Isotopic evidence for an aerobic nitrogen cycle in the latest Archean. *Science* **323**, 1045–1048 (2009).
- Reinhard, C. T., Raiswell, R., Scott, C., Anbar, A. D. & Lyons, T. W. A late Archean sulfidic sea stimulated by early oxidative weathering of the continents. *Science* **326**, 713–716 (2009).
- Duan, Y. et al. Molybdenum isotope evidence for mild environmental oxygenation before the Great Oxidation Event. *Geochim. Cosmochim. Acta* **74**, 6655–6668 (2010).
- Kendall, B., Creaser, R. A., Reinhard, C. T., Lyons, T. W. & Anbar, A. D. Transient episodes of mild environmental oxygenation and oxidative continental weathering during the late Archean. *Sci. Adv.* **1**, e1500777 (2015).
- Gregory, D. D. et al. The chemical conditions of the late Archean Hamersley Basin inferred from whole rock and pyrite geochemistry with $\Delta 33\text{S}$ and $\delta 34\text{S}$ isotope analyses. *Geochim. Cosmochim. Acta* **149**, 223–250 (2015).
- Wille, M. et al. Evidence for a gradual rise of oxygen between 2.6 and 2.5 Ga from Mo isotopes and Re-PGE signatures in shales. *Geochim. Cosmochim. Acta* **71**, 2417–2435 (2007).
- Algeo, T. J. & Tribouillard, N. Environmental analysis of paleoceanographic systems based on molybdenum-uranium covariation. *Chem. Geol.* **268**, 211–225 (2009).
- Johnson, J. E. et al. Manganese-oxidizing photosynthesis before the rise of cyanobacteria. *Proc. Natl Acad. Sci. USA* **110**, 11238–11243 (2013).
- Anbar, A. D. & Holland, H. D. The photochemistry of manganese and the origin of banded iron formations. *Geochim. Cosmochim. Acta* **56**, 2595–2603 (1992).
- Kendall, B., Dahl, T. W. & Anbar, A. D. Good golly, why Moly? The stable isotope geochemistry of molybdenum. *Rev. Mineral. Geochem.* **82**, 682–732 (2017).
- Nielsen, S. G., Rehkämper, M. & Prytulak, J. Investigation and application of thallium isotope fractionation. *Rev. Mineral. Geochem.* **82**, 759–798 (2017).
- Holland, H. D. *The Chemical Evolution of the Atmosphere and Oceans* (Princeton Univ. Press, Princeton, 1984).
- Häbicht, K. S., Gade, M., Thamdrup, B., Berg, P. & Canfield, D. E. Calibration of sulfate levels in the Archean ocean. *Science* **298**, 2372–2374 (2002).
- De Kock, M. O., Evans, D. A. D. & Beukes, N. J. Validating the existence of Vaalbara in the Neoproterozoic. *Precamb. Res.* **174**, 145–154 (2009).
- Madison, A. S., Tebo, B. M., Mucci, A., Sundby, B. & Luther, G. W. III Abundant porewater Mn(III) is a major component of the sedimentary redox system. *Science* **341**, 875–878 (2013).

Acknowledgements

We would like to thank W. Zheng and J. Blusztajn for their help with instrumental analysis at Arizona State University and the Woods Hole Oceanographic Institution, respectively. This research was supported financially by the NSF Frontiers in Earth System Dynamics programme (award no. NSF EAR-1338810), the NSF Chemical Oceanography programme (award no. OCE 1434785), the NASA Exobiology programme (award no. NNX16AJ60G), an NSERC Discovery Grant (award no. RGPIN-435930) and the NASA Astrobiology Institute (award no. NNA15BB03A). This material is based on work supported by the National Science Foundation Graduate Research Fellowship Program under grant no. 026257-001. Any opinions, findings, and conclusions or recommendations expressed in this material are those of the authors and do not necessarily reflect the views of the National Science Foundation.

Author contributions

C.M.O., S.G.N., J.D.O., B.K., and A.D.A. developed the project idea. C.M.O. processed samples and performed Tl and Mo isotope analyses with contributions from S.G.N.,

J.D.O., B.K., G.W.G. and S.J.R. C.M.O. performed the modelling and wrote the manuscript with contributions from all co-authors.

Competing interests

The authors declare no competing interests.

Additional information

Supplementary information is available for this paper at <https://doi.org/10.1038/s41561-019-0309-7>.

Reprints and permissions information is available at www.nature.com/reprints.

Correspondence and requests for materials should be addressed to C.M.O.

Publisher's note: Springer Nature remains neutral with regard to jurisdictional claims in published maps and institutional affiliations.

© The Author(s), under exclusive licence to Springer Nature Limited 2019

Methods

Tl isotopes. Tl sample preparation and purification were performed in the NIRVANA Laboratory at Woods Hole Oceanographic Institution (WHOI), as well as in J. Owens' Laboratory at Florida State University within the National High Magnetic Field Laboratory (NHMFL). Powdered samples from ABDP9 were leached using a method from the literature^{17,20}, which has been shown to effectively separate authigenic Tl (that is Tl bound to pyrite) from detrital Tl. Each fraction was subsequently digested following procedures discussed in that literature. Ion exchange chromatography was completed using previously described techniques^{51,52}. Similar to recent work²⁰, samples were only subjected to one column pass because Tl concentrations were high and thus very little sample mass was processed.

Tl isotopic analyses were conducted at the WHOI Plasma Mass Spectrometry Facility and at the NHMFL in Tallahassee. At both locations a Thermo Neptune multi-collector inductively coupled plasma mass spectrometer (MC-ICPMS) was used with an Aridus II desolvating nebulizer sample introduction system. Measurements were made in low-resolution mode utilizing sample-standard bracketing relative to NIST 997 Tl in epsilon notation. External normalization to NIST SRM 981 Pb was utilized to monitor instrumental mass bias, similar to previous studies^{51,52}. As a known quantity of NIST SRM 981 Pb was added to each sample, Tl concentrations could be calculated during MC-ICPMS analysis using the measured ²⁰⁵Tl/²⁰⁸Pb ratios. Tl isotope values are reported in epsilon notation relative to NIST 997 Tl metal. One USGS shale SCO-1 standard was leached, purified, and analysed with each sample set to monitor accuracy and showed good reproducibility ($\epsilon^{205}\text{Tl}_{\text{authigenic}} = -2.80 \pm 0.13$, 2 s.d., $n = 8$) compared to a recent study (-2.92 ± 0.11)²⁰.

Mo isotopes. All Mo sample digestion, isotope purification and analysis was completed at the W.M. Keck Foundation Laboratory for Environmental Biogeochemistry at Arizona State University. Quarter cores were cut from ABDP9, powdered, ashed and digested; concentrations were then analysed using the same techniques employed in previous work³⁴. A large enough sample was then taken from the same digested stock solutions to provide 125 ng Mo that was spiked with an optimal amount of calibrated synthetic Mo isotope double-spike (⁹⁷Mo and ¹⁰⁰Mo) before purification via ion exchange chromatography, again utilizing methods from previous studies^{53,54}. The double spike is used for chromatography and instrumental mass fractionation correction.

Isotope ratio measurements were performed on a Thermo Neptune MC-ICPMS in low-resolution mode with an Elemental Scientific Inc. Apex inlet system and using sample-standard bracketing^{38,55}. All measurements were made using the Johnson Matthey Specpure Mo plasma standard (Lot no. 802309E; Roch-Mo2) as the bracketing standard, and then re-calculated relative to the new international NIST SRM 3134 standard = +0.25‰ (ref. ²⁶). Samples and standards were analysed at a concentration of 25 $\mu\text{g g}^{-1}$ Mo, which yielded about 3 V of signal on mass 98. Samples were analysed in triplicate (at least), with the average 2 s.d. sample reproducibility being 0.06‰, and the maximum being 0.11‰. Over the 12-month period of Mo isotope analysis for this study, USGS rock reference material SDO-1 was simultaneously processed with each batch of samples to monitor accuracy and showed good reproducibility ($\delta^{98}\text{Mo} = 1.00 \pm 0.09\text{‰}$ (2 s.d.) compared with $1.05 \pm 0.14\text{‰}$ from a previous study⁵⁶), as did various analytical

Table 1 | Standard solution $\delta^{98}\text{Mo}$ values from this study versus previous work

Standard	This study (‰) ^a	<i>n</i>	Normalized to NIST + 0.25‰ (‰) ^b	Goldberg et al. ⁵⁶ (‰)
Roch-Mo2	Bracketing standard		-0.09	-0.09 ± 0.05
ICL-Mo	0.16 ± 0.03	38	0.07 ± 0.03	0.09 ± 0.05
Kyoto-Mo	-0.04 ± 0.05	39	-0.13 ± 0.05	-0.12 ± 0.06
NIST SRM 3134	0.33 ± 0.06	45	0.24 ± 0.06	0.25 (reporting standard)
SDO-1	1.12 ± 0.05	45	1.03 ± 0.05	1.05 ± 0.14

^aMeasured relative to Roch-Mo2. ^bNormalized using $\delta^{98}\text{Mo}_{\text{Roch-Mo2}} = -0.09\text{‰}$ relative to $\delta^{98}\text{Mo}_{\text{NIST+0.25‰}}$ (ref. ⁵⁶). All reported errors are 2 s.d. of the standard reproducibility.

replicates (Table 1). Lastly, for each analytical run, a series of standards with varying spike/sample ratios was measured. All samples were within the validated spike/sample range for accurate and precise $\delta^{98}\text{Mo}$ values.

Data availability

All data generated during this study are included in the Supplementary Information.

References

- Rehkämper, M. & Halliday, A. N. The precise measurement of Tl isotopic compositions by MC-ICPMS: applications to the analysis of geological materials and meteorites. *Geochim. Cosmochim. Acta* **63**, 935–944 (1999).
- Nielsen, S. G., Rehkämper, M., Baker, J. A. & Halliday, A. N. The precise and accurate determination of thallium isotope compositions and concentrations for water samples by MC-ICPMS. *Chem. Geol.* **204**, 109–124 (2004).
- Siebert, C., Nägler, T. F. & Kramers, J. D. Determination of the molybdenum isotope fractionation by double-spike multicollector inductively coupled plasma mass spectrometry. *Geochem. Geophys. Geosyst.* **2**, 2000GC000124 (2001).
- Barling, J., Arnold, G. L. & Anbar, A. D. Natural mass-dependent variations in the isotopic composition of molybdenum. *Earth Planet. Sci. Lett.* **193**, 447–457 (2001).
- Kendall, B., Creaser, R. A., Gordon, G. W. & Anbar, A. D. Re-Os and Mo isotope systematics of black shales from the Middle Proterozoic Velkerri and Wollogorang Formations, McArthur Basin, northern Australia. *Geochim. Cosmochim. Acta* **73**, 2534–2558 (2009).
- Goldberg, T. et al. Resolution of inter-laboratory discrepancies in Mo isotope data: an intercalibration. *J. Anal. Atom. Spectrom.* **28**, 724–735 (2013).